

## Electronic Supplementary Information

### **Evaluation of Histone Deacetylase Inhibitor Substituted Zinc and Indium Phthalocyanines for Chemo- and Photodynamic Therapy**

Başak Aru<sup>a,b</sup>, Aysel Günay<sup>c</sup>, Gülderen Yanıkkaya Demirel<sup>b\*</sup>, Ayşe Gül Gürek<sup>c\*</sup>, and Devrim Atilla<sup>c\*</sup>

<sup>a</sup> *Department of Molecular Biology and Genetics, Gebze Technical University, 41400 Gebze, Kocaeli, Turkey.*

<sup>b</sup> *Faculty of Medicine, Immunology Department, Yeditepe University, 34755 Ataşehir, İstanbul, Turkey.*

<sup>c</sup> *Department of Chemistry, Gebze Technical University, 41400 Gebze, Kocaeli, Turkey.*

**Equation S1.**

$$\text{Viability (\%)} = \frac{(O_2 \times A_1) - (O_1 \times A_2)}{(O_2 \times P_1) - (O_1 \times P_2)} \times 100$$

- O1 = molar extinction coefficient of oxidized AB at 570 nm (80586)
- O2 = molar extinction coefficient of oxidized AB at 600 nm (117216)
- A1 = absorbance of test wells at 570 nm
- A2 = absorbance of test wells at 600 nm
- P1 = absorbance of positive control well (cells plus Alamar Blue but no test agent) at 570 nm
- P2 = absorbance of positive control well (cells plus Alamar Blue but no test agent) at 600 nm



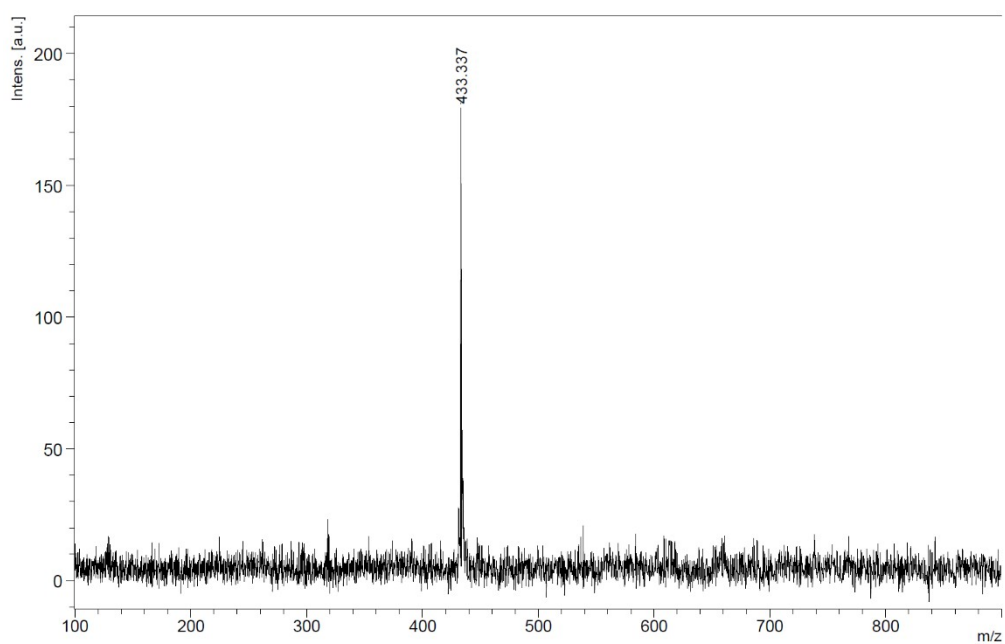


Figure S3: Mass spectrum of compound 3a.

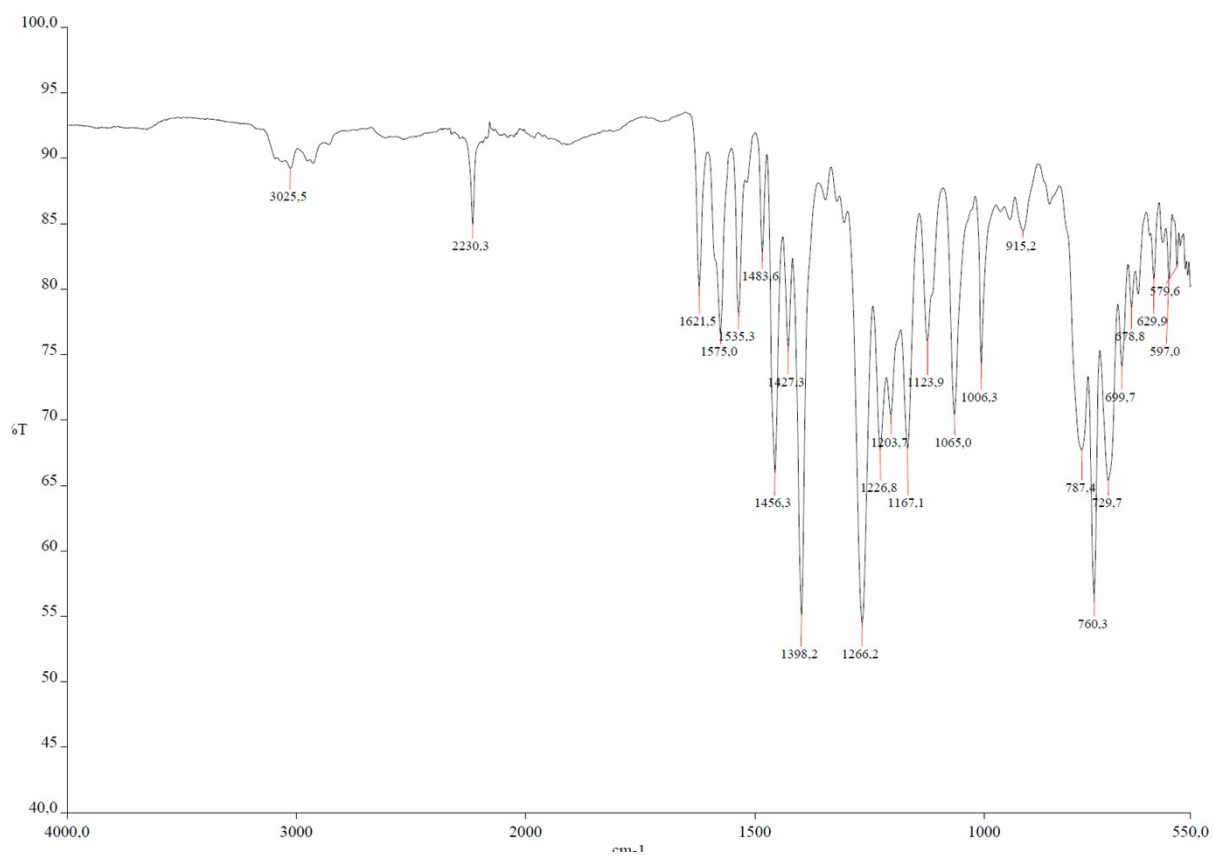


Figure S4: IR spectrum of compound 3a.

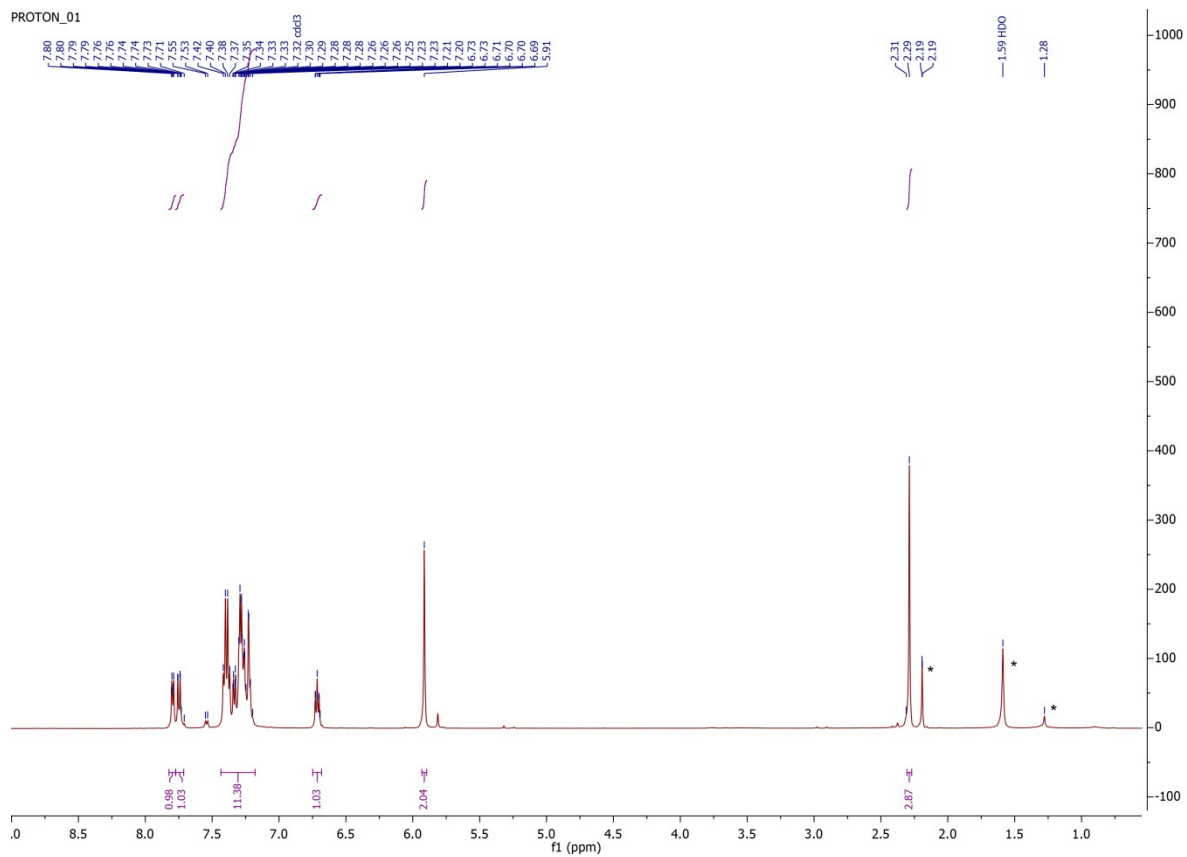


Figure S5:  $^1\text{H-NMR}$  spectrum of compound **3b** (in  $d\text{-CDCl}_3$ , \*ethanol, water, and acetone as residual)

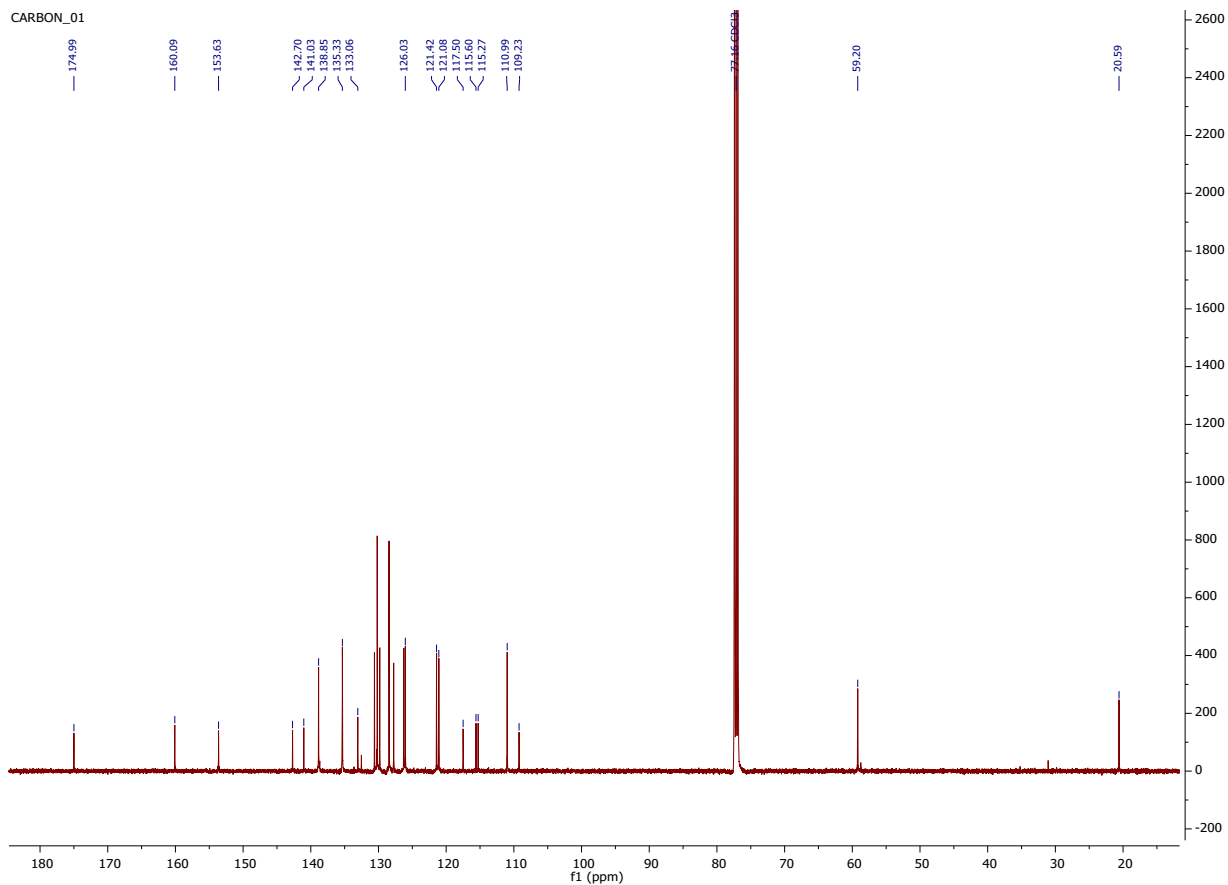


Figure S6:  $^{13}\text{C}$ NMR spectrum of compound **3b** (in  $d\text{-CDCl}_3$ ).

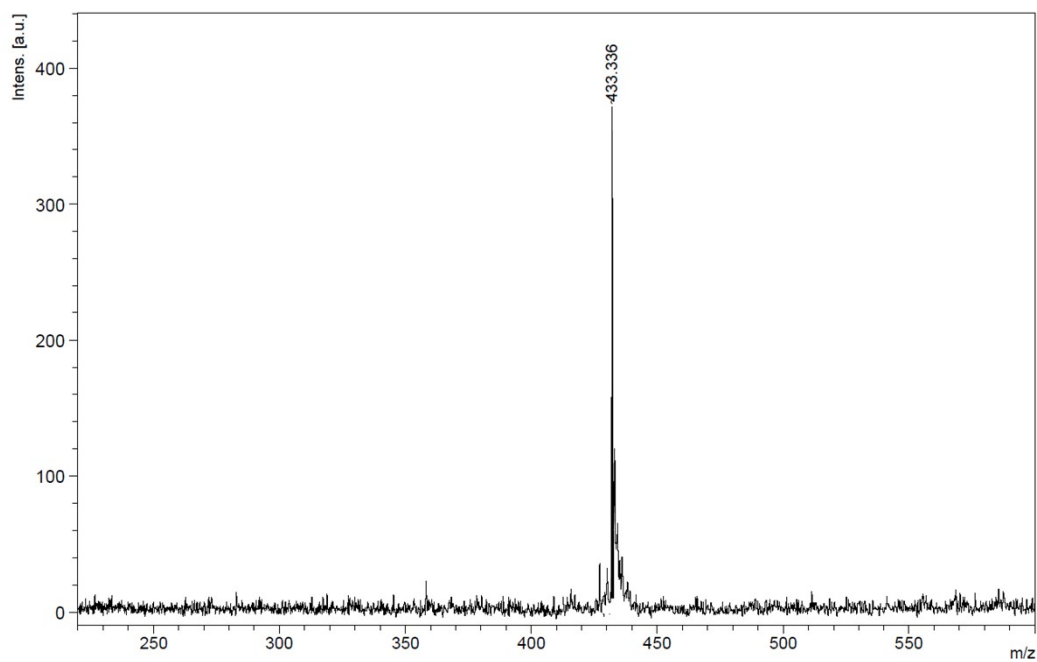


Figure S7: Mass spectrum of compound **3b**.

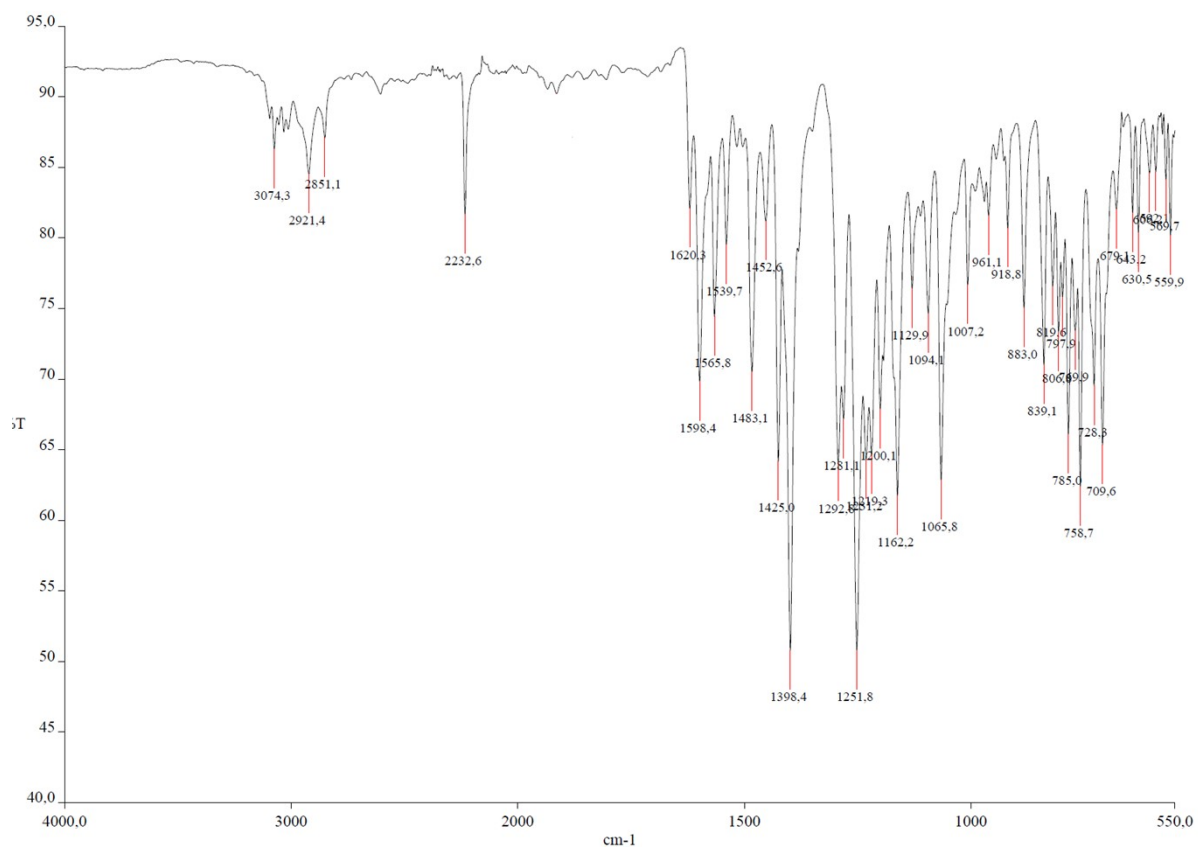


Figure S8: IR spectrum of compound **3a**.

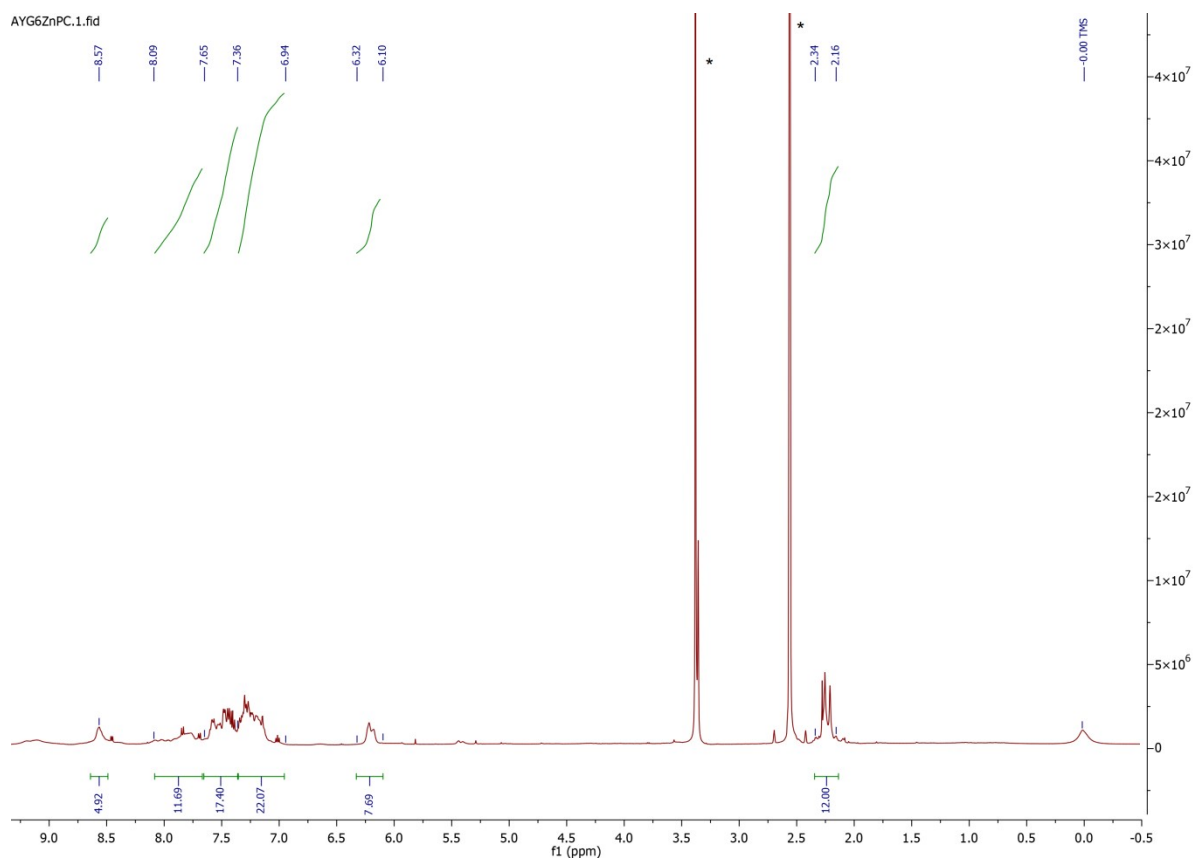


Figure S9:  $^1\text{H}$ -NMR spectrum of **ZnPc-1** ( $*d_6$ -DMSO and water)

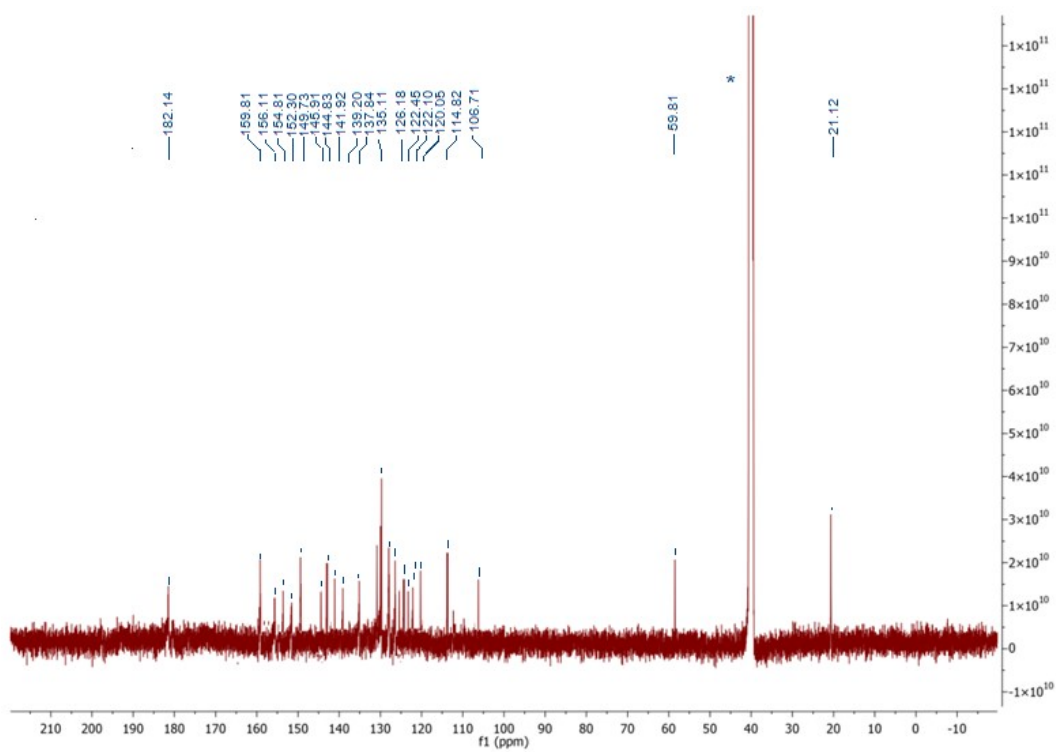


Figure S10:  $^{13}\text{C}$ -NMR spectrum of **ZnPc-1** ( $*d_6$ -DMSO)



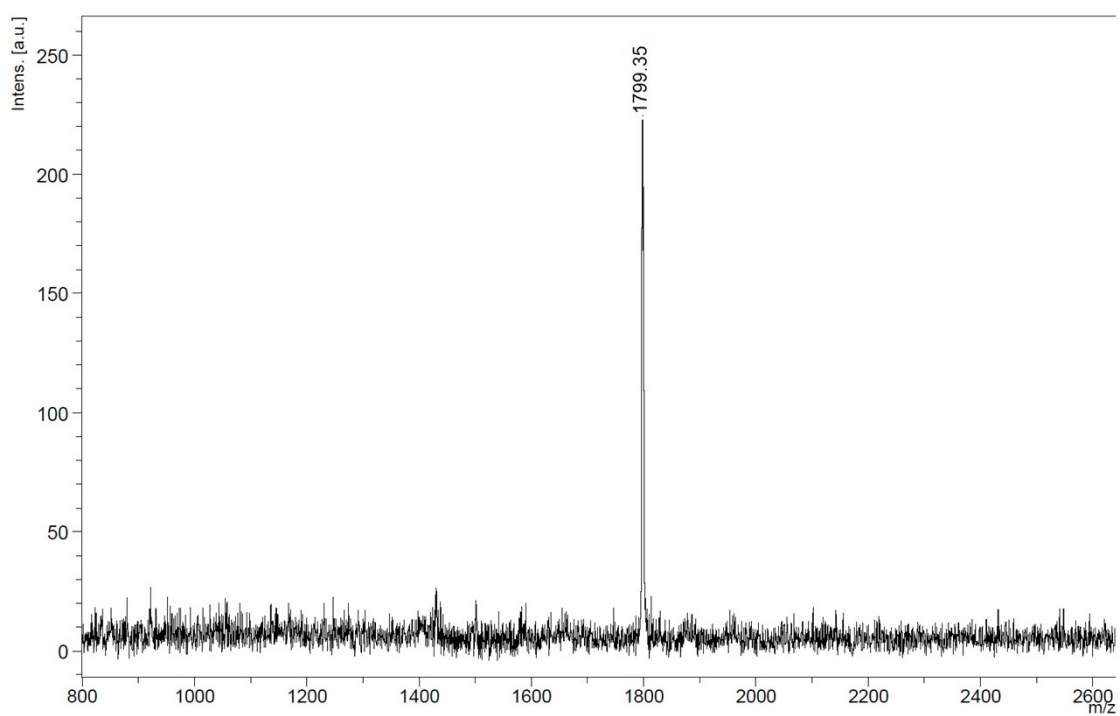


Figure S11: Mass spectrum of **ZnPc-1**.

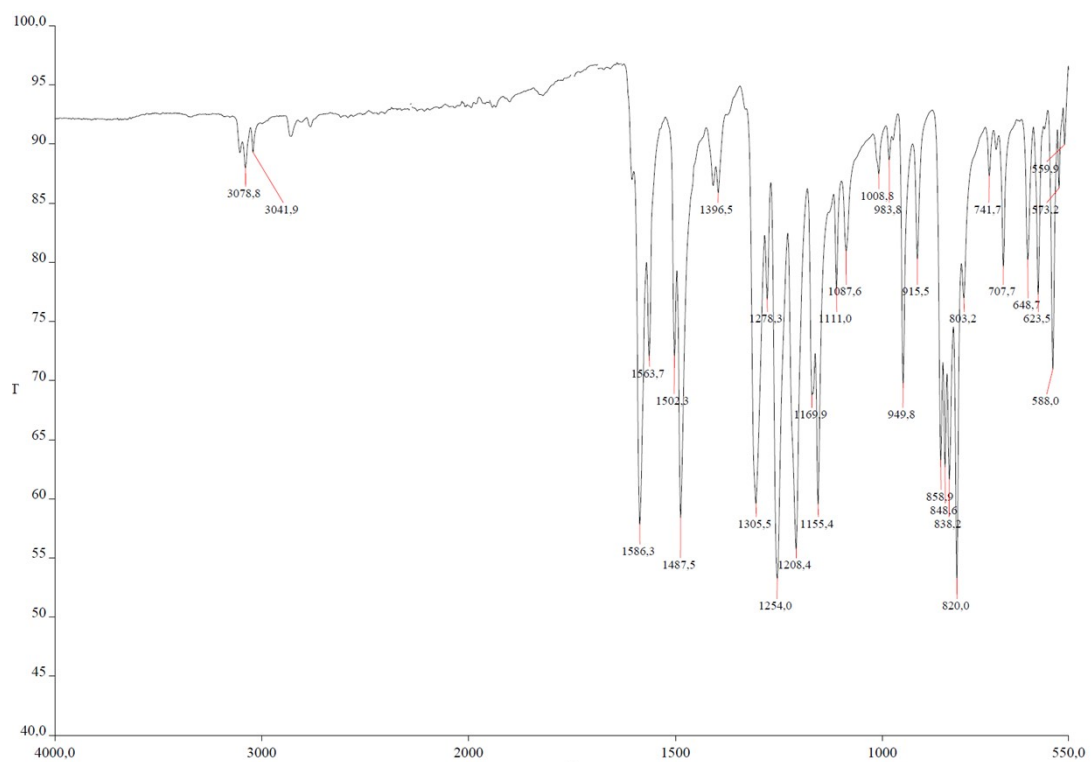


Figure S12: IR spectrum of **ZnPc-1**.

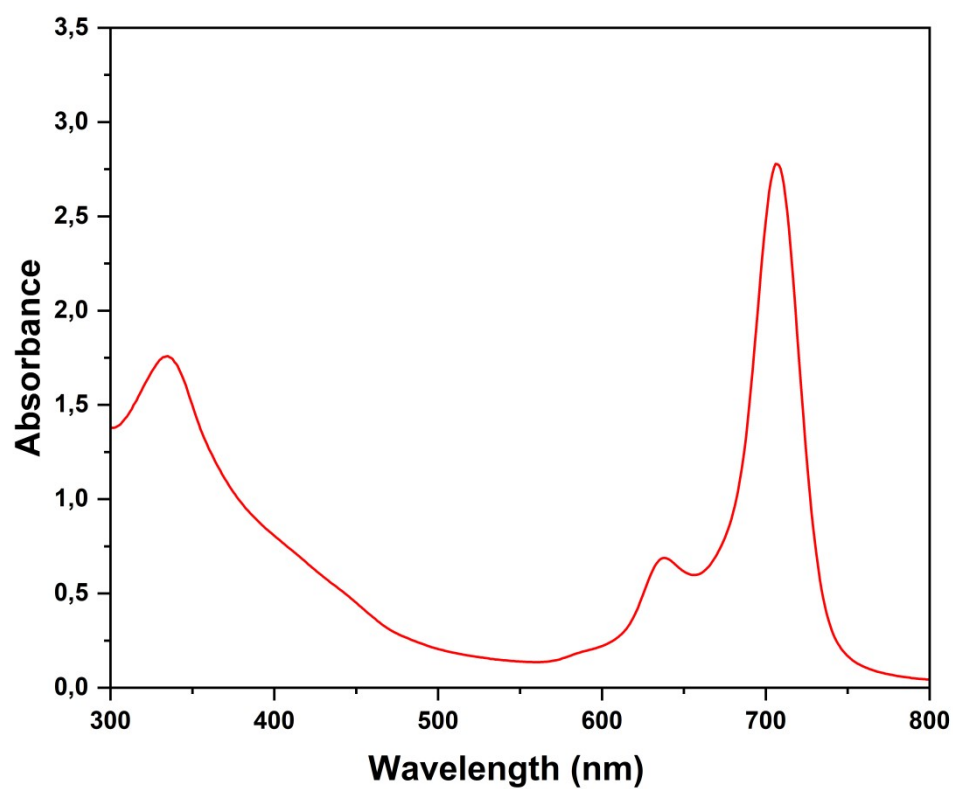


Figure S13: UV-Vis spectrum of **ZnPc-1** (in DMSO,  $1.5 \times 10^{-5}$  M)

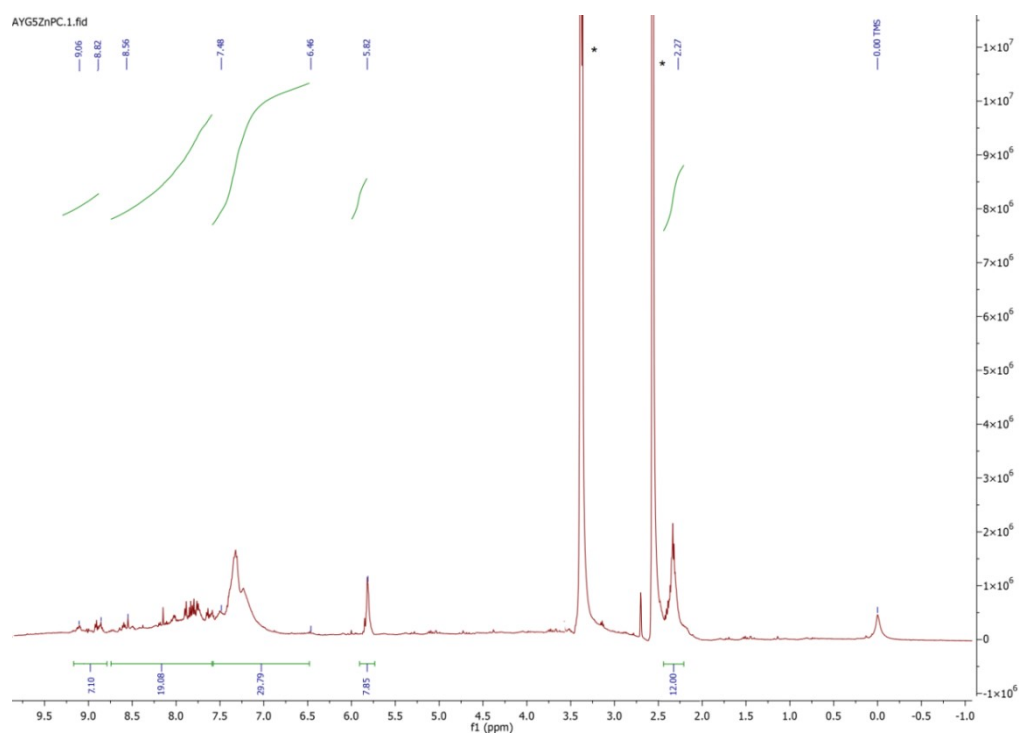


Figure S14:  $^1\text{H}$ -NMR spectrum of **ZnPc-2**. (\* $d_6$ -DMSO, water)

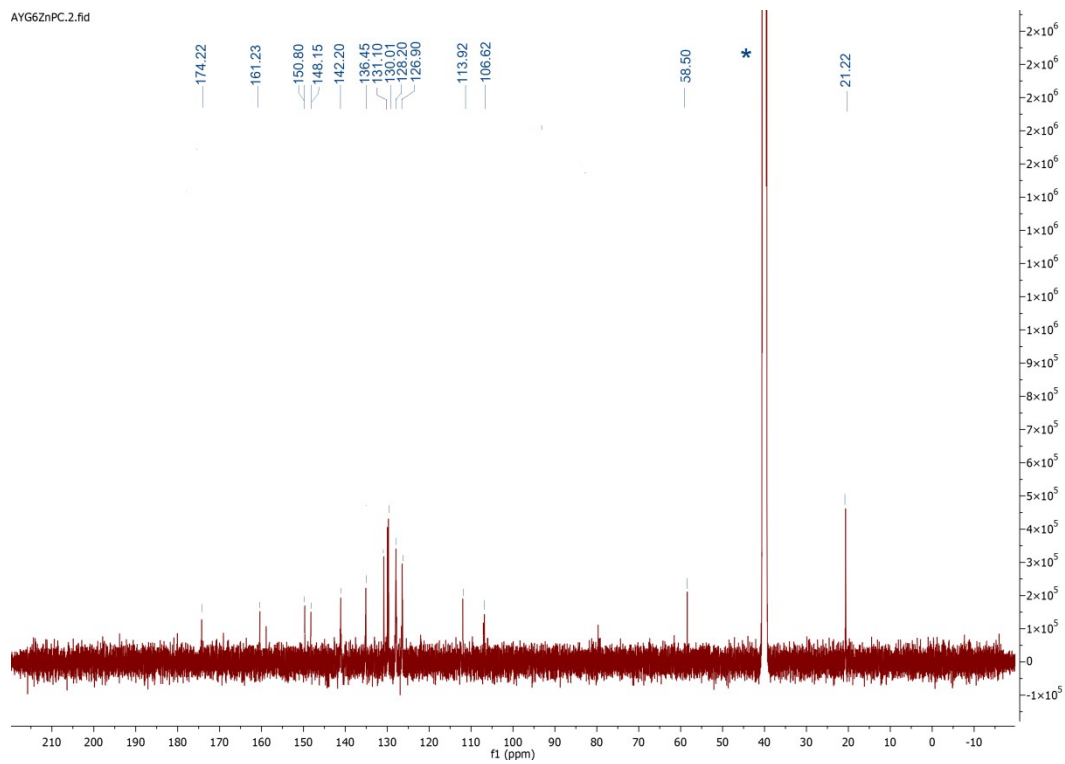


Figure S15:  $^{13}\text{C}$ -NMR spectrum of **ZnPc-2** ( $d_6$ -DMSO).

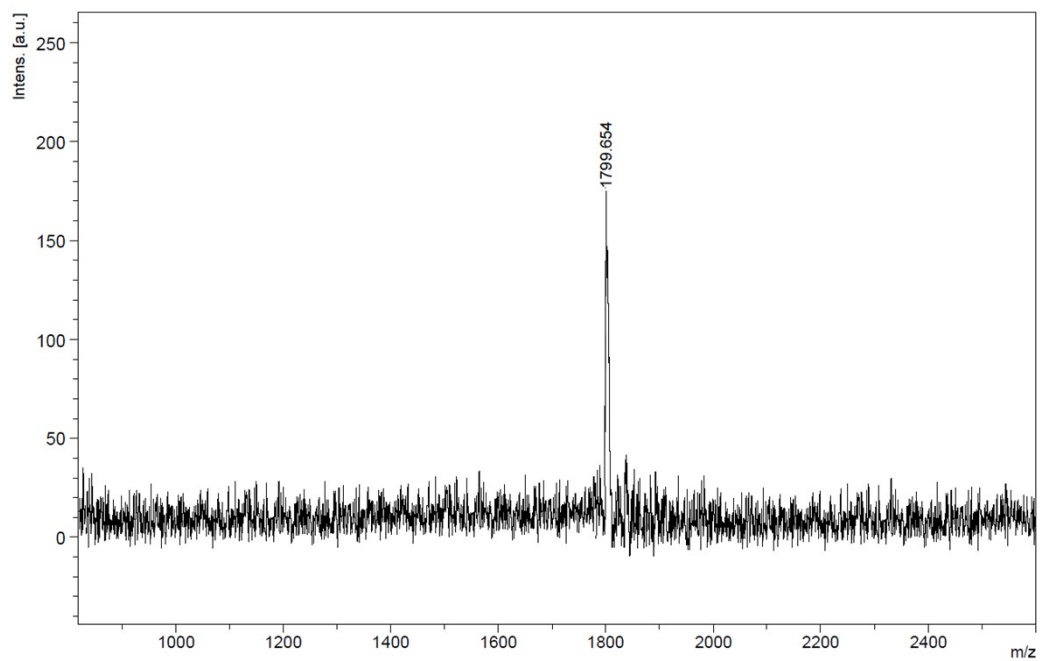


Figure S16: Mass spectrum of **ZnPc-2**.

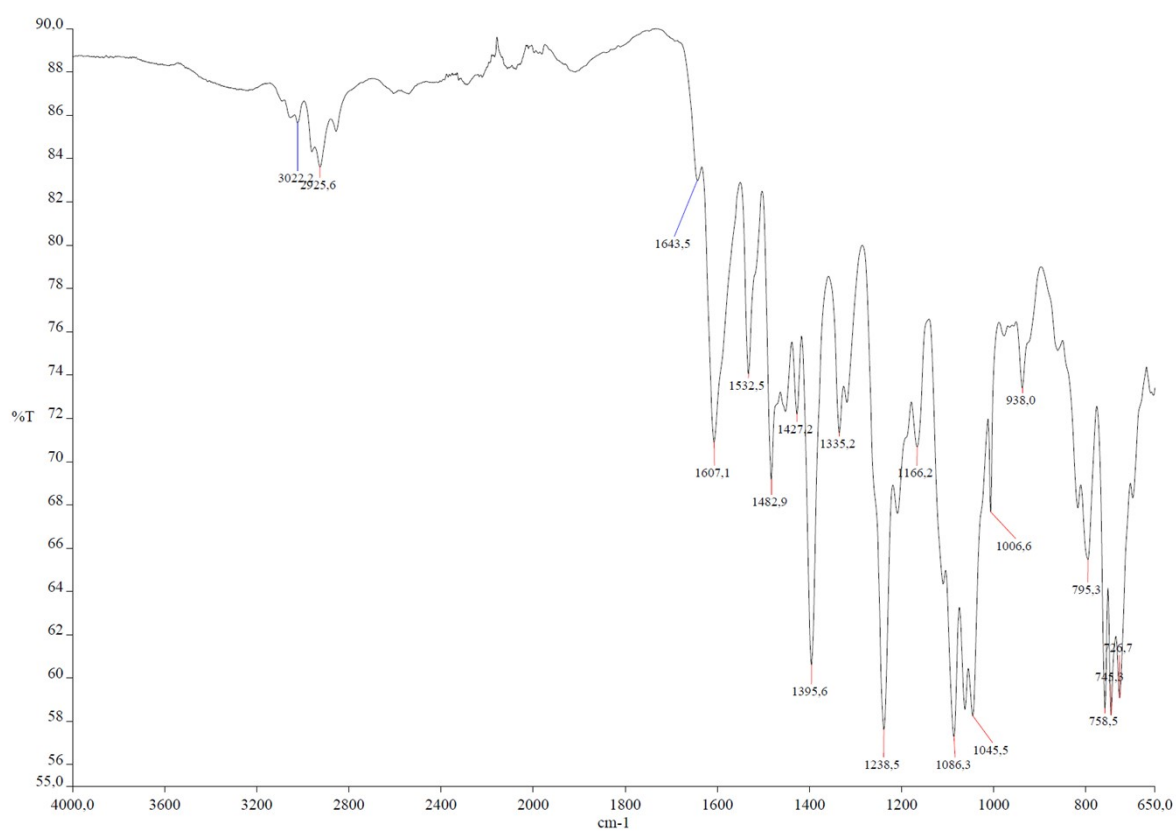


Figure S17: IR spectrum of **ZnPc-2**.

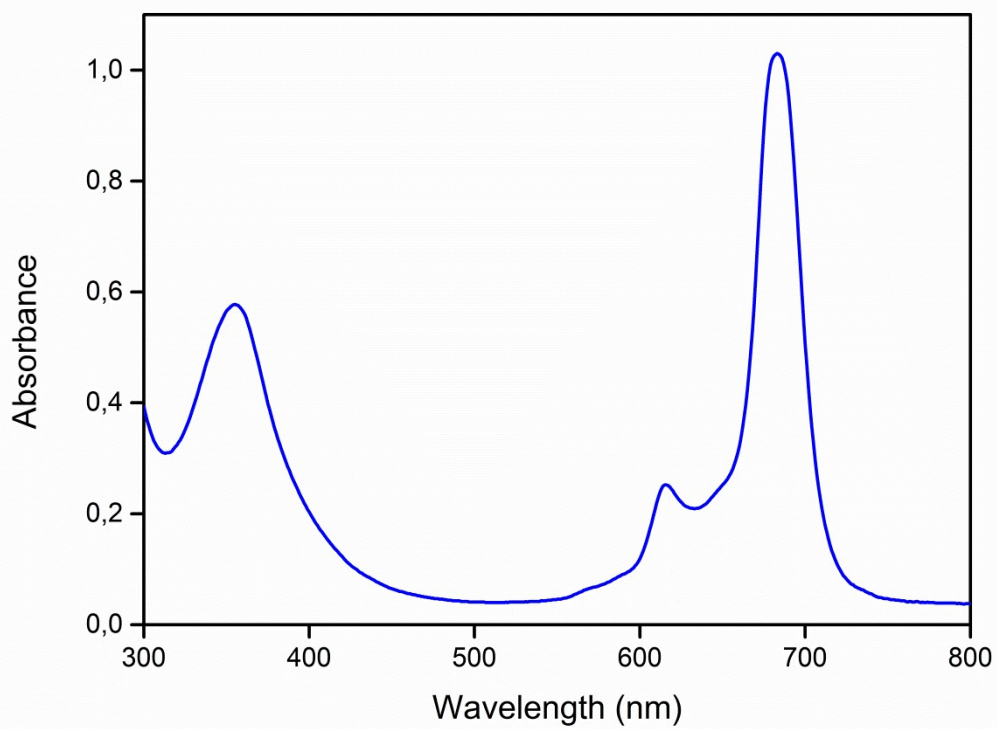


Figure S18: UV-Vis spectrum of **ZnPc-2** (in DMSO,  $6.0 \times 10^{-6}$  M).

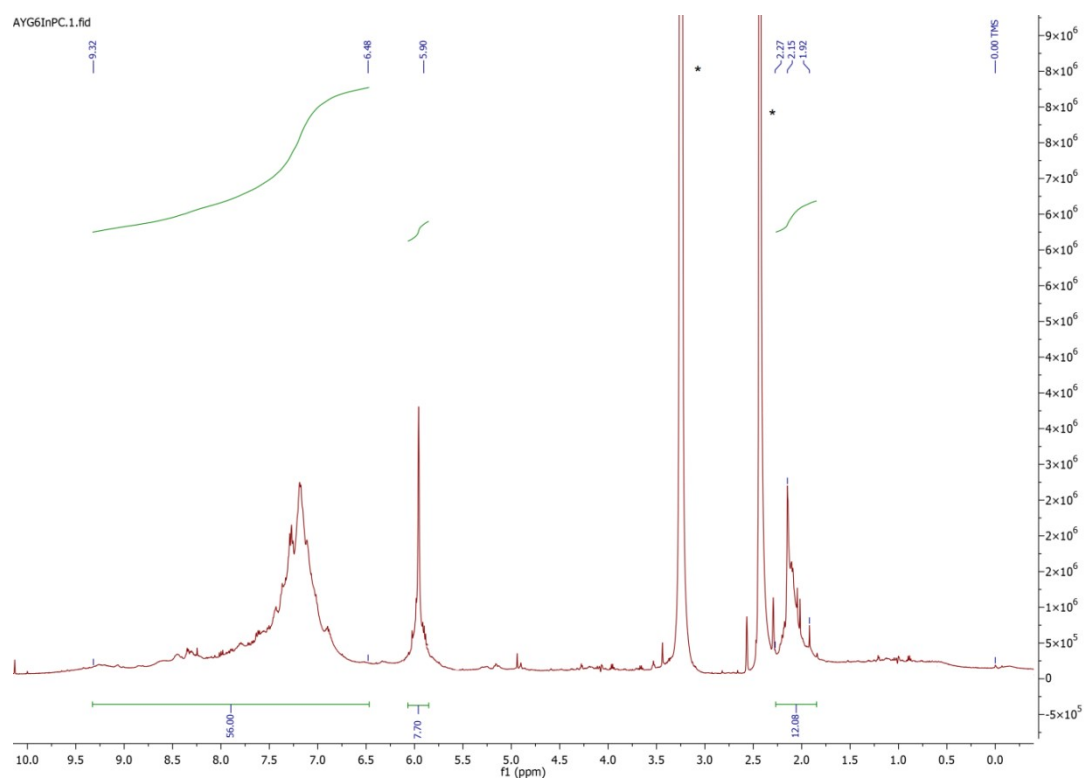


Figure S19: <sup>1</sup>H-NMR spectrum of **InPc-1** (\**d*<sub>6</sub>-DMSO and water).

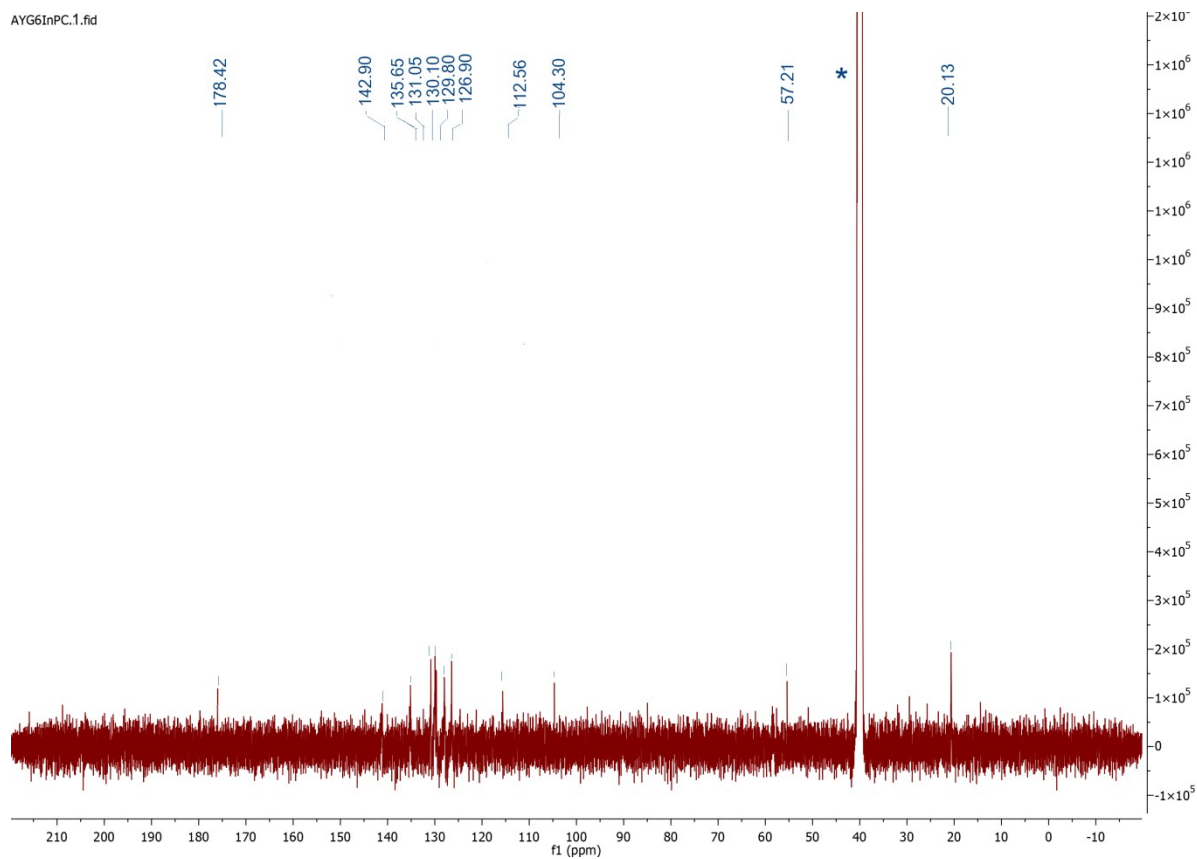


Figure S20: <sup>13</sup>C-NMR spectrum of **InPc-1** (\**d*<sub>6</sub>-DMSO).

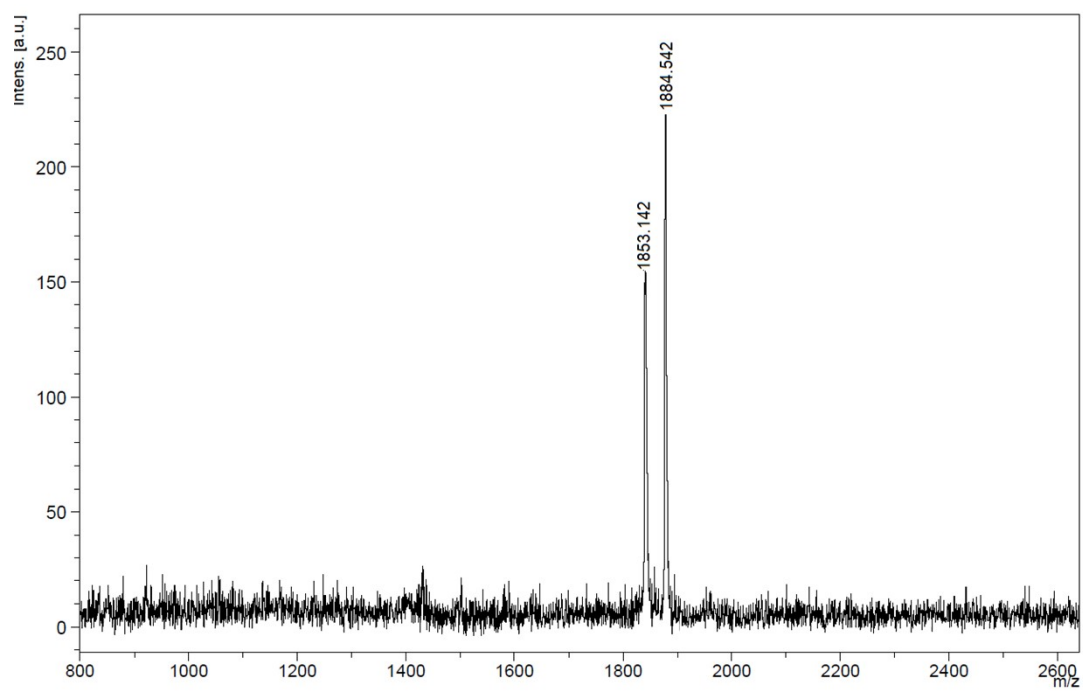


Figure S21: Mass spectrum of InPc-1.

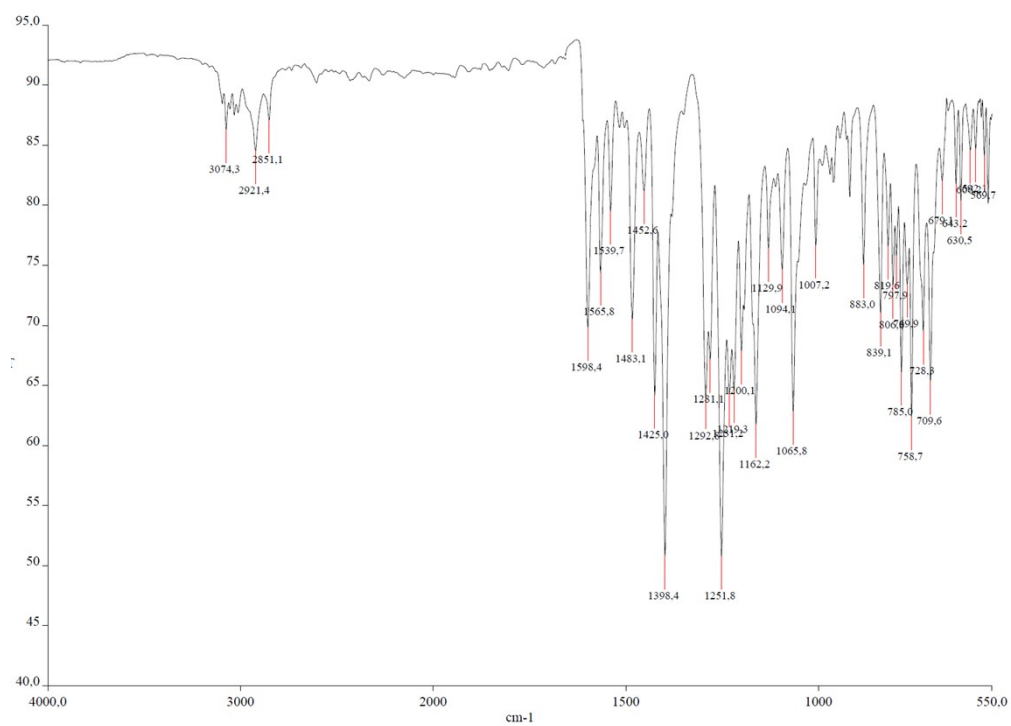


Figure S22: IR spectrum of InPc-1.

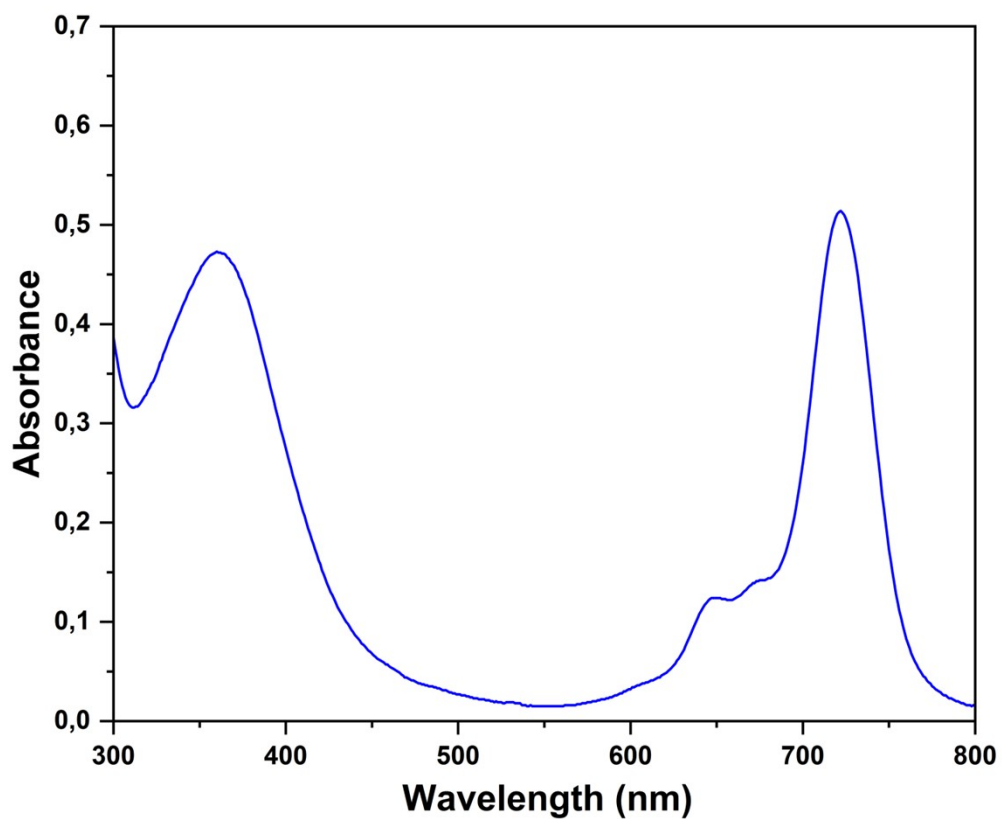


Figure S23: UV-Vis spectrum of **InPc-1** (in DMSO).

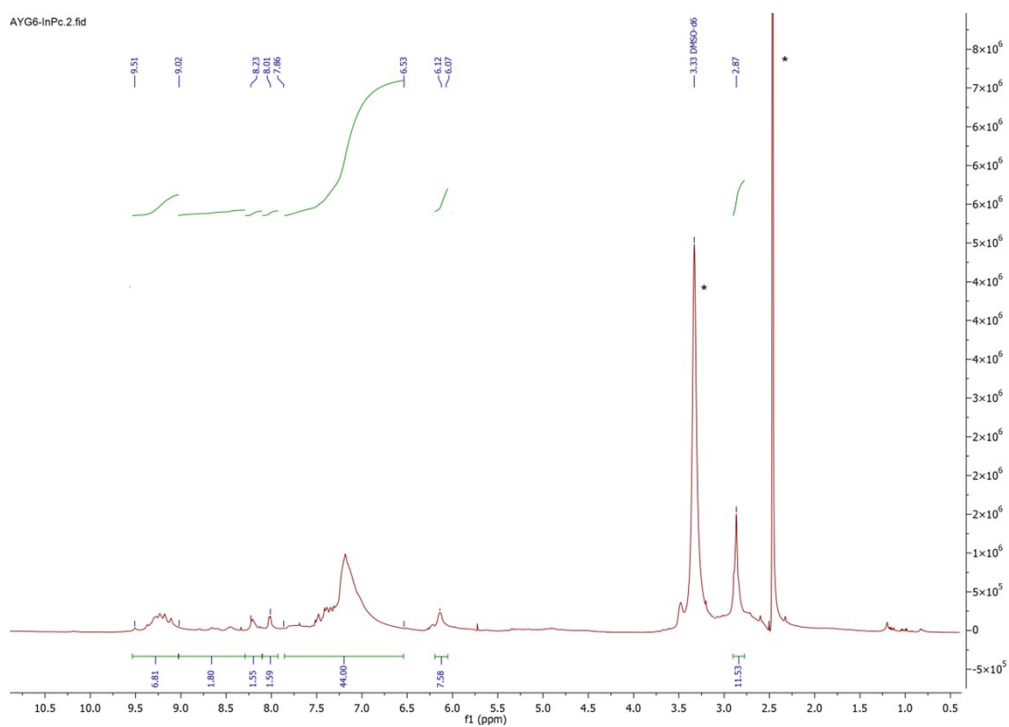


Figure S24: <sup>1</sup>H-NMR spectrum of **InPc-2** (\**d*<sub>6</sub>-DMSO and water).



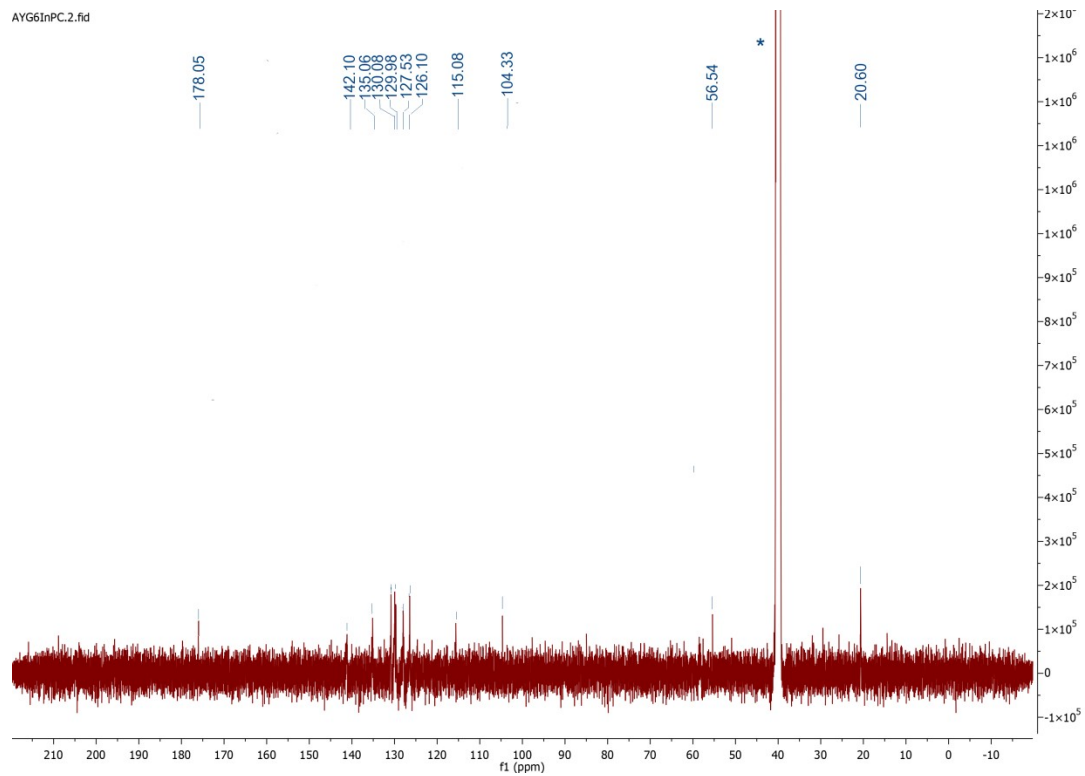


Figure S25:  $^{13}\text{C}$ -NMR spectrum of **InPc-2** ( $d_6$ -DMSO).

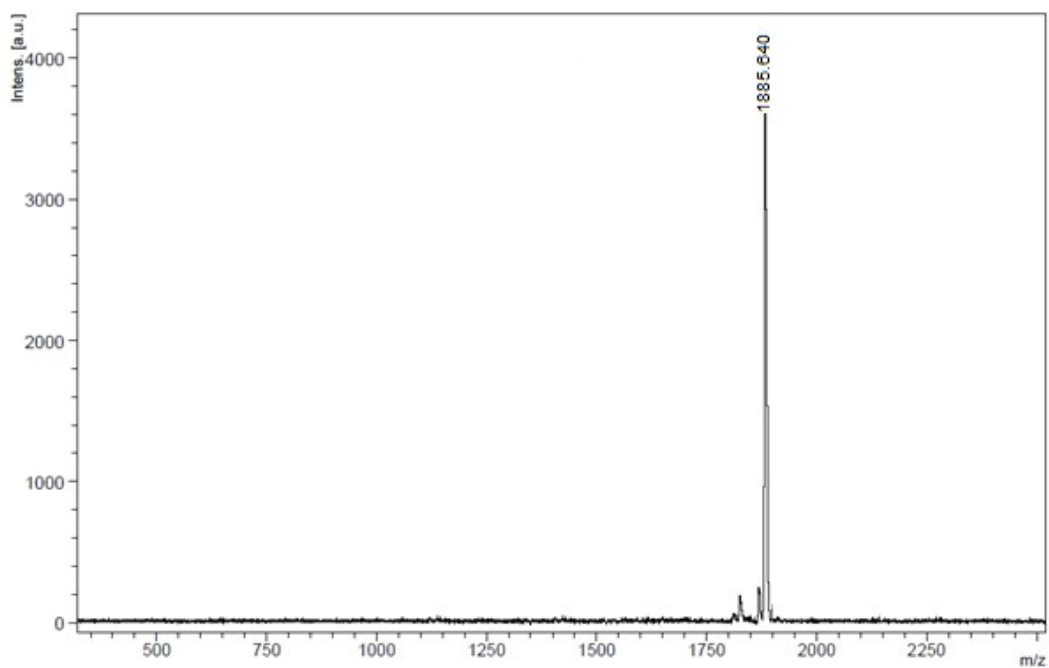


Figure S26: Mass spectrum of **InPc-2**.

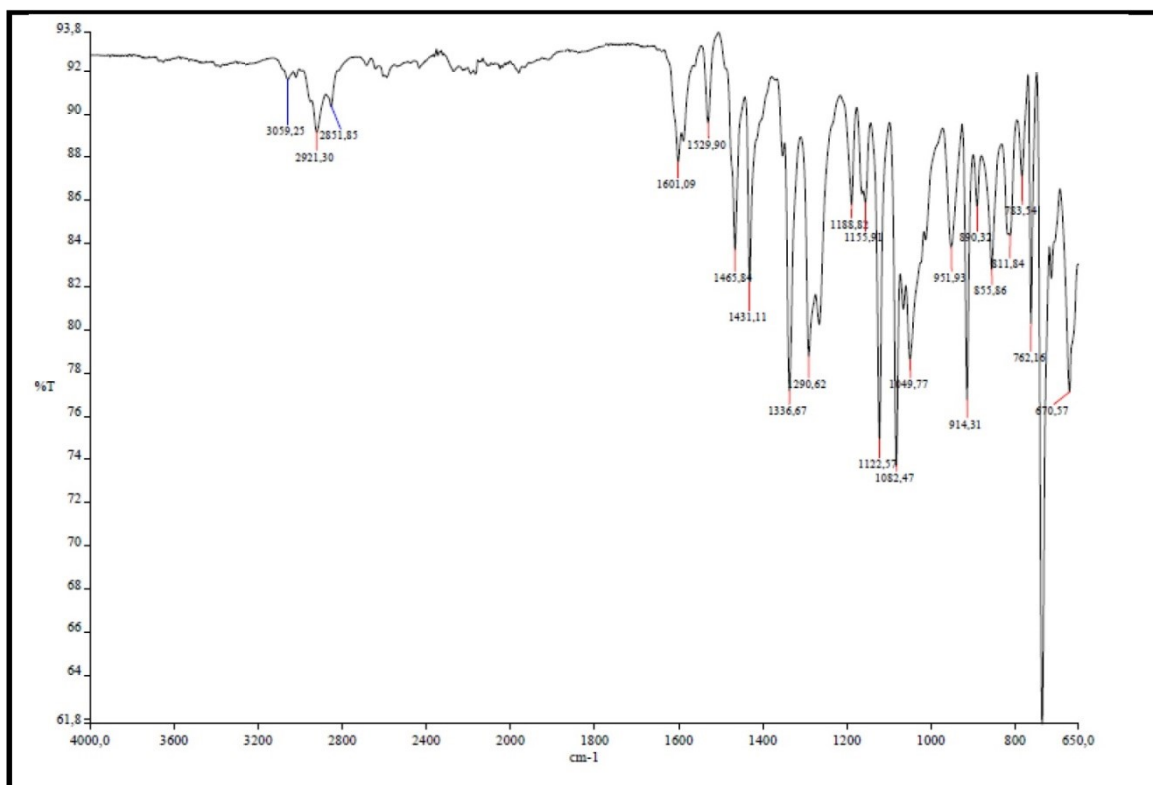


Figure S27: IR spectrum of **InPc-2**.

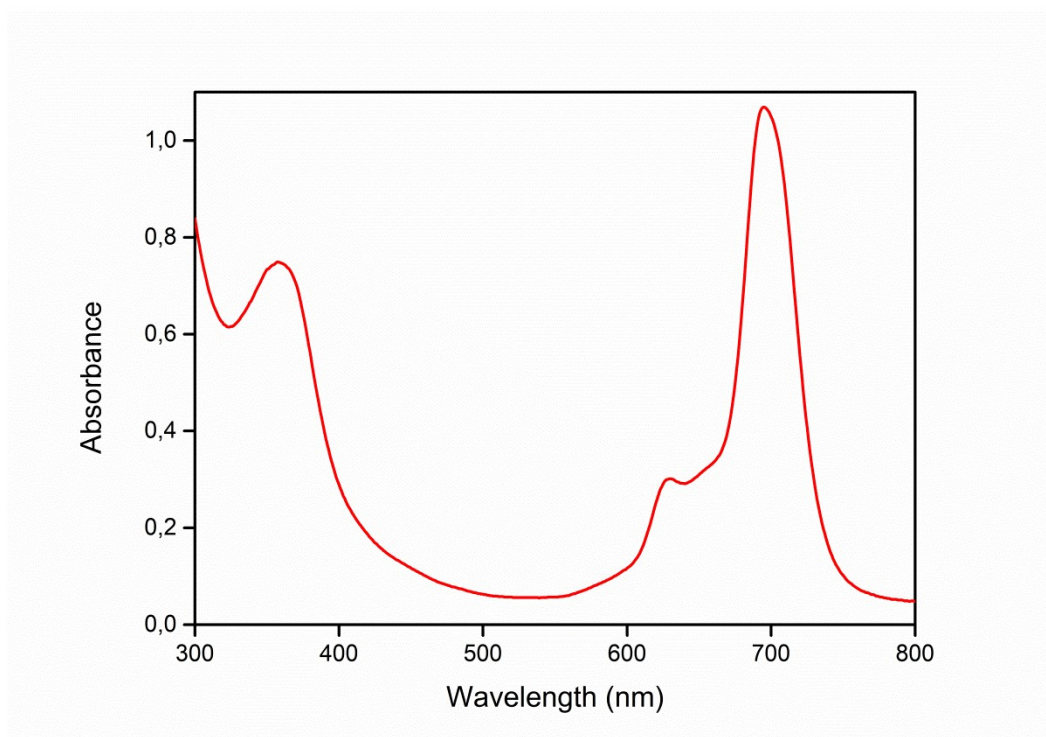


Figure S28: UV-Vis spectrum of **InPc-2**(in DMSO,  $4.2 \times 10^{-6}$ M).

## Photochemistry

The photochemical (singlet oxygen generation) properties of were investigated in comparison with unsubstituted zinc(II)phthalocyanine (**ZnPc**) as standart in DMF. All of the data discussed below are summarized in Table S1.

### Singlet oxygen quantum yield ( $\Phi_{\Delta}$ ) determination

For direct method, the calculation of the  $^1\text{O}_2$  quantum yields was based on the detection of NIR  $^1\text{O}_2$  luminescence by an optical method based on the comparison of single molecular oxygen phosphorescence produced by the Pc sample with that generated by the reference ZnPc in the near infrared region at 1276 nm.  $\Phi_{\Delta}$  values were calculated according to Equation S2.

$$\Phi_{\Delta s} = \Phi_{\Delta r} \frac{\eta_s^2 A_r I_s}{\eta_r^2 A_s I_r} \quad (\text{S2})$$

In Eq. S2,  $\Phi_{\Delta s}$  and  $\Phi_{\Delta r}$  are the quantum yields of the sample and reference and  $\eta_s$  and  $\eta_r$  are refractive indexes of the solvents used for the measurements of the sample and reference.  $A_s$  and  $A_r$  are the absorbance of the sample and the reference, and  $I_s$  and  $I_r$  are the integrated areas under the emission spectra of the sample and the reference, respectively.

Table S1. Singlet oxygen quantum yield ( $\Phi_{\Delta}$ ) of **ZnPc-1**, **ZnPc-2**, **InPc-1** and **InPc-2** phthalocyanine complexes.

Compounds	Indirect $\Phi_{\Delta}$ in DMF
<b>ZnPc-1</b>	0.57
<b>InPc-1</b>	0.57
<b>ZnPc-2</b>	0.73
<b>InPc-2</b>	0.50

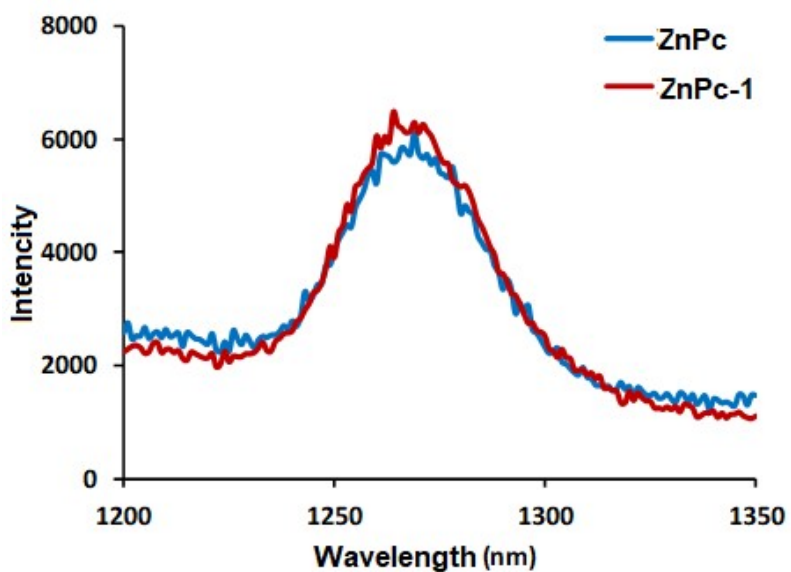


Figure S29. Singlet oxygen phosphorescence with sensitization in DMF from **ZnPc-1** and ZnPc.

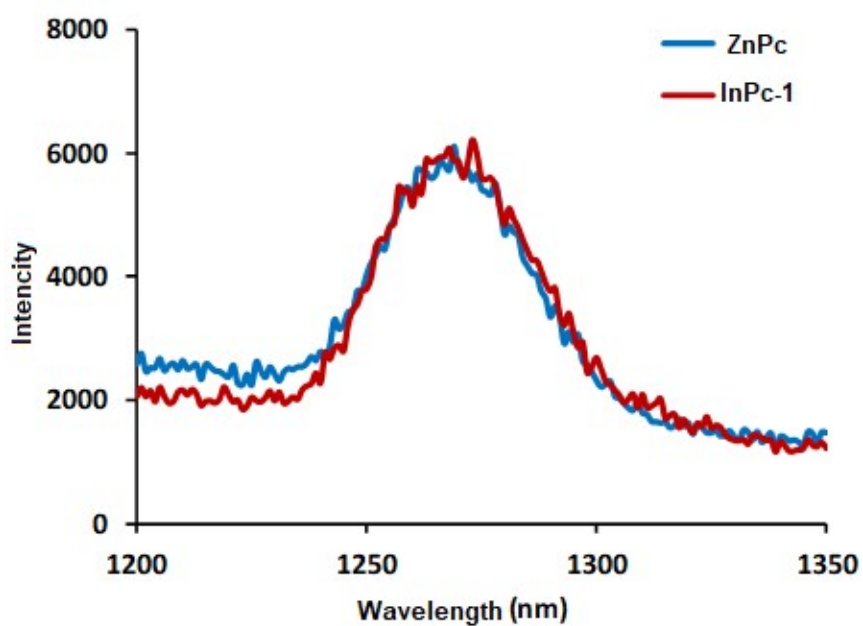


Figure S30. Singlet oxygen phosphorescence with sensitization in DMF from **InPc-1** and ZnPc.

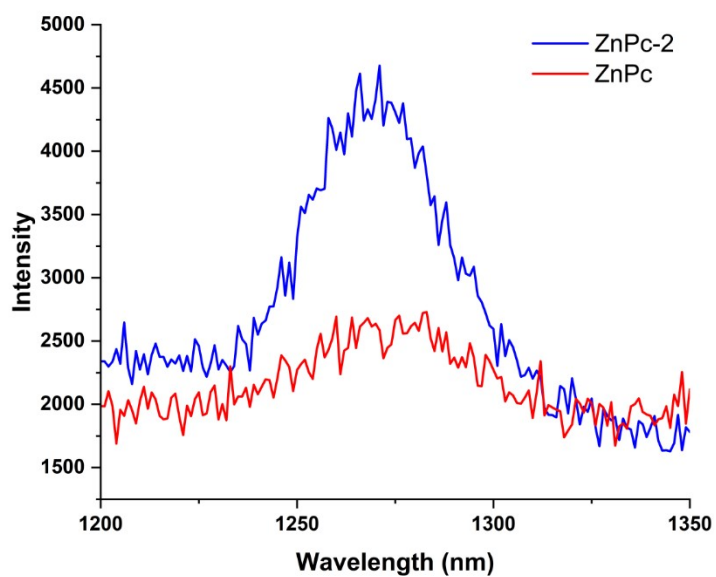


Figure S31. Singlet oxygen phosphorescence with sensitization in DMF from **ZnPc-1** and ZnPc.

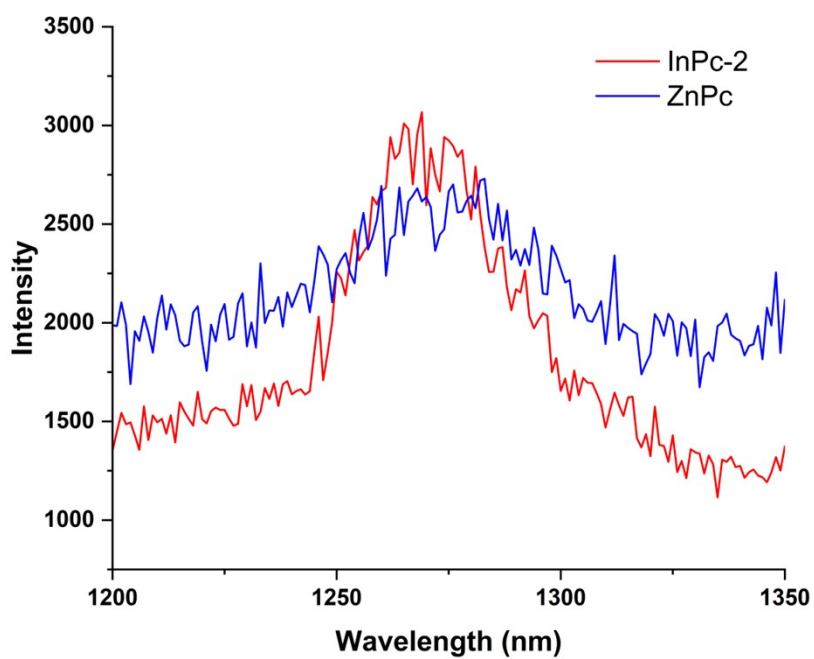


Figure S32. Singlet oxygen phosphorescence with sensitization in DMF from **InPc-2** and ZnPc.

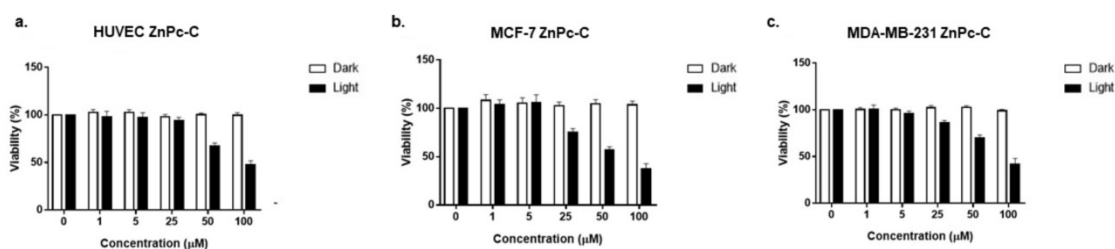


Figure S33: Bar graphics indicating cytotoxic properties of **ZnPc-C**. Measurements were performed after incubating cells with compounds for 24 hours under dark conditions, and after irradiating cells and further incubating for an additional 24 hours. a. HUVEC, b. MCF-7, c. MDA-MB-231.

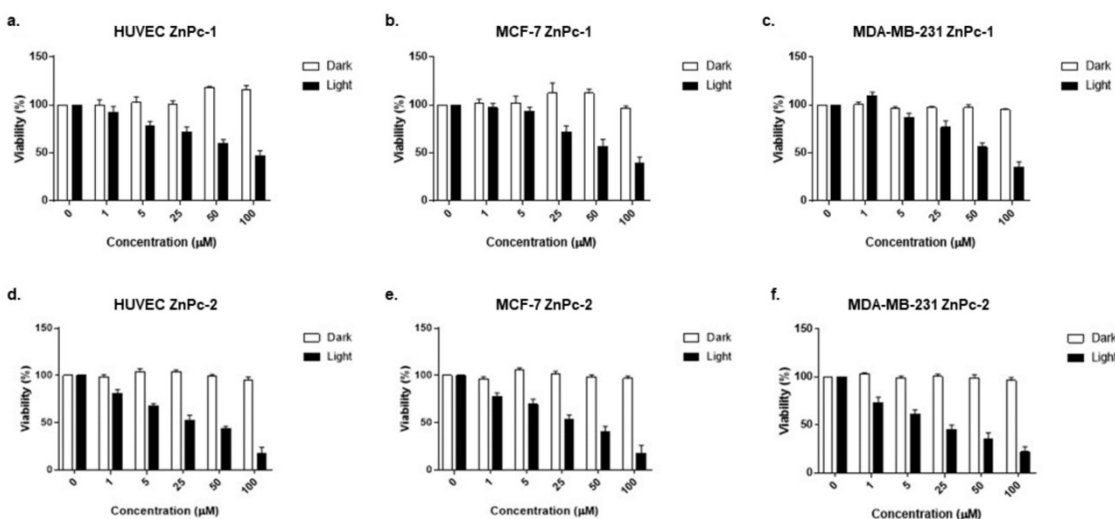


Figure S34: Bar graphics indicating cytotoxic properties of **ZnPc-1** and **ZnPc-2**. Measurements were performed after incubating cells with compounds for 24 hours under dark conditions, and after irradiating cells and further incubating for an additional 24 hours. Both **ZnPc-1** (a-c) (non-peripheral) and **ZnPc-2** (peripheral) (d-f) did not influence viability on HUVECs, MCF-7 and MDA-MB-231 cell lines while decreasing viability upon irradiation in a dose dependent manner. Each test was done as triplicates.

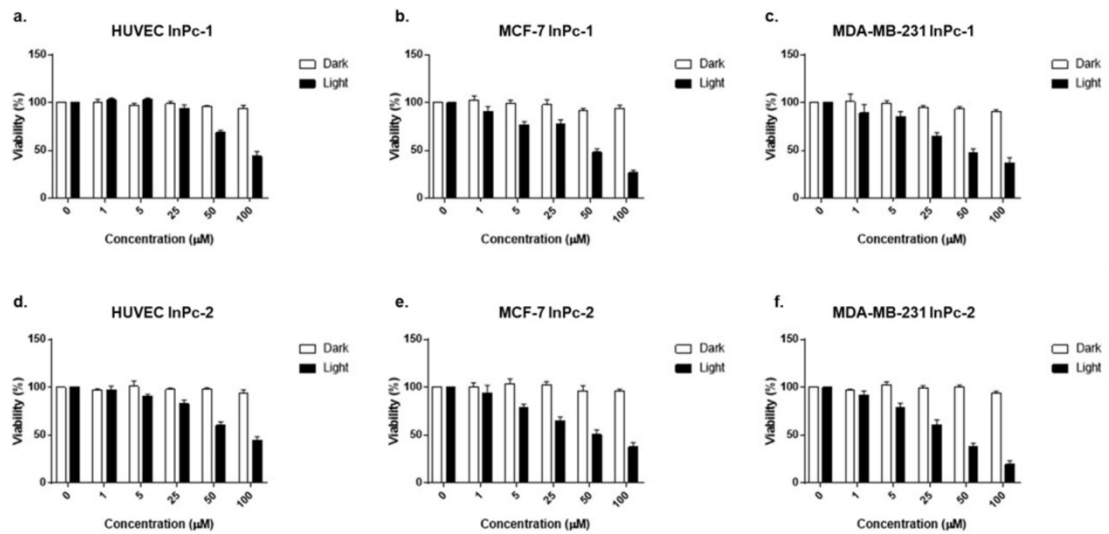


Figure S35: Bar graphics indicating cytotoxic properties of **InPc-1** and **InPc-2**. Measurements were performed after incubating cells with compounds for 24 hours under dark conditions, and after irradiating cells and further incubating for an additional 24 hours. Both **InPc-1** (a-c) (non-peripheral) and **InPc-2** (peripheral) (d-f) did not influence viability on HUVECs, MCF-7 and MDA-MB-231 cell lines while decreasing viability upon irradiation in a dose dependent manner. Each test was done as triplicates.

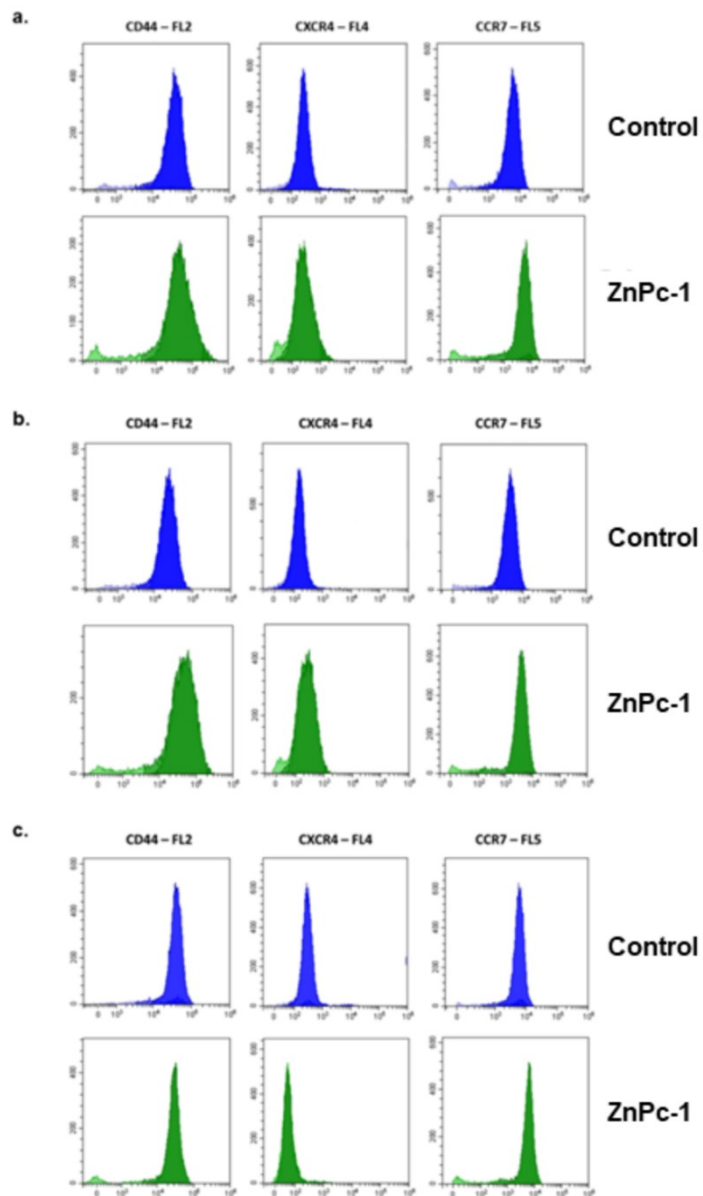


Figure S36: Representative flow cytometry histograms demonstrating CD44, CXCR4 and CCR7 protein levels of untreated and **ZnPc-1** treated a. HUVECs, b. MCF-7 cells, c. MDA-MB-231 cells.



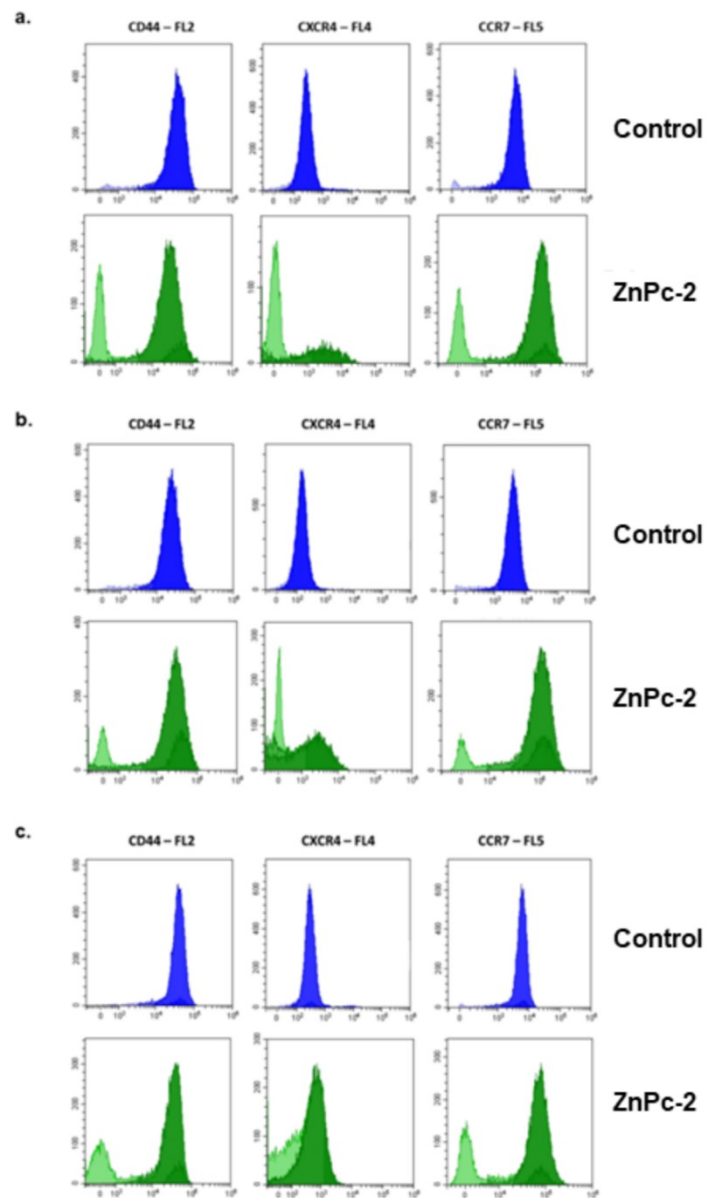


Figure S37: Representative flow cytometry histograms demonstrating CD44, CXCR4 and CCR7 protein levels of untreated and **ZnPc-2** treated a. HUVECs, b. MCF-7 cells, c. MDA-MB-231 cells.

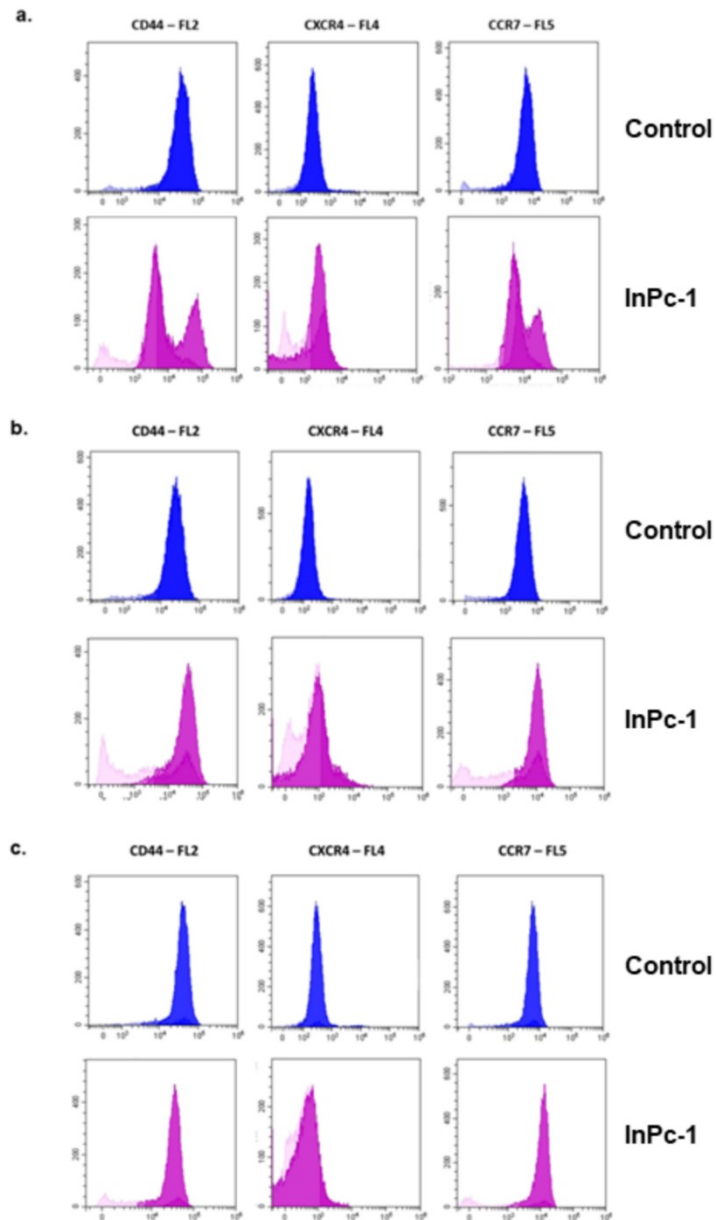


Figure S38: Representative flow cytometry histograms demonstrating CD44, CXCR4 and CCR7 protein levels of untreated and **InPc-1** treated a. HUVECs, b. MCF-7 cells, c. MDA-MB-231 cells.

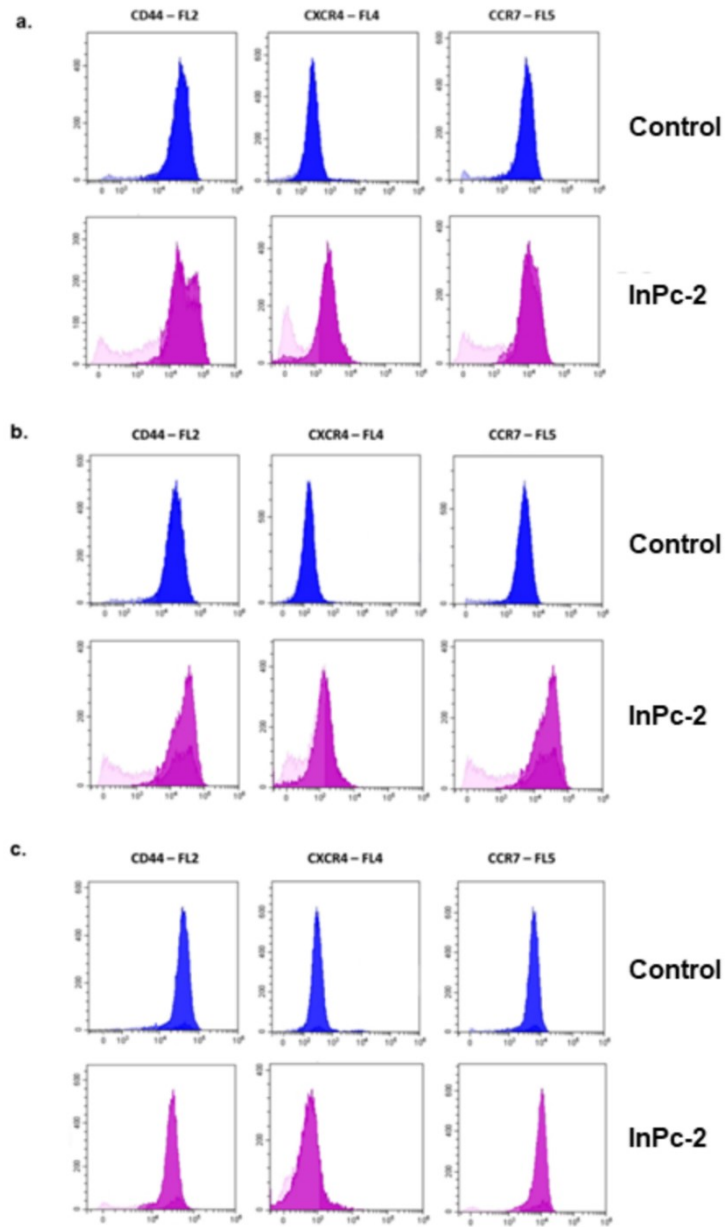


Figure S39: Representative flow cytometry histograms demonstrating CD44, CXCR4 and CCR7 protein levels of untreated and **InPc-2** treated a. HUVECs, b. MCF-7 cells, c. MDA-MB-231 cells.